1

Measurement Systems and Parameters for CO_2 Photo/Electro-Conversion

Li Li, Zhenwei Zhao, Xinyi Wang, and Zhicheng Zhang

Tianjin University, School of Science, Department of Chemistry, Tianjin Key Laboratory of Molecular Optoelectronic Sciences, No. 92, Weijin road, Nankai district, Tianjin, 300072, China

1.1 Introduction

Fossil fuels are the main fuels in today's society, whose combustion produces a large amount of CO_2, bringing a series of environmental pollution problems. The capture and conversion of carbon dioxide have become the focus of current research. It is important to convert CO_2 into chemicals and fuels with higher added values, which can alleviate environmental pollution and energy problems. CO_2 photo/electric conversion can use renewable clean energy to convert CO_2, becoming the most potential conversion method. Here, we summarized the measurement systems and parameters for CO_2 photo/electro-conversion, which mainly include photocatalysis, electrocatalysis, and photo-electro-catalysis systems.

1.2 The Measurement Systems for CO_2 Photo/Electro-Conversion

In the chapter, we mainly introduce three photo/electro conversion systems, namely photocatalytic CO_2 reduction, electrocatalytic CO_2 reduction, and photo-electro-catalytic CO_2 reduction. The main purpose of this chapter is to explain how to test catalysts and evaluate their advantages and disadvantages, so as to provide readers with a more comprehensive and systematic summary.

1.2.1 The Measurement Systems of Photocatalytic CO_2 Reduction

Generally, photocatalytic CO_2 reduction reaction systems are mainly divided into two categories: under liquid-phase reaction system and in gas-phase reaction system.

CO_2 Conversion and Utilization: Photocatalytic and Electrochemical Methods and Applications, First Edition. Edited by Zhicheng Zhang.

1.2.1.1 CO_2 Reduction System Under Liquid-Phase Reaction System

(1) Definition of liquid-phase reaction system: The liquid-phase reaction system refers to the reduction reaction occurring in the saturated solution of CO_2, and the photocatalyst can be uniformly dispersed in the solution.
(2) Characteristics of liquid-phase reaction system: In the liquid-phase reaction system, because the solid catalyst dispersed in the solution is always in the agitated state, its charge transfer efficiency and heat transfer efficiency are higher. However, in the liquid-phase reaction system, the limited solubility and diffusion coefficient of CO_2 in H_2O will limit the mass transfer efficiency of the photocatalytic CO_2 reduction reaction. Under the reaction conditions of 25 °C and 101.325 kPa, the solubility of CO_2 in H_2O is less than 0.033 mol L^{-1}, which weakens the diffusion of CO_2 molecules from the gas phase to the photocatalyst surface. Compared with neutral and acidic conditions, the solubility of CO_2 under alkaline conditions is higher. The solubility of CO_2 can be improved by increasing the pH value of the solution, or organic solvents such as acetonitrile (ACN) and ethyl acetate (EAA) can be added to H_2O to promote the dissolution of CO_2.
(3) General reaction device of liquid-phase reaction system: In the CO_2 reduction reaction experiment in the liquid-phase system, 300 W xenon lamp light source (which can also be replaced according to the specific experimental test needs) is generally used to simulate solar radiation, and filter or light intensity meter can be used to adjust the appropriate light wavelength and light intensity [1]. The whole reaction system is generally carried out at room temperature (special reactions can also be adjusted as required). The specific operations are as follows: weigh a certain amount of catalyst and ultrasonically disperse it in a specific solvent (select according to different materials). Pour its dispersion into a closed device, and inject 99.9% CO_2 into it. After 30 minutes, to ensure that the rest of the interfering gas is discharged, close the reaction device. Put the reaction system under the xenon lamp and turn on the condensing device or other thermostatic devices to ensure that the system is at a certain temperature. The timing starts when the light source is turned on, and the gas samples in the system are collected at certain intervals as required to facilitate the subsequent determination of products.

1.2.1.2 CO_2 Reduction System in Gas-Phase Reaction System

(1) Definition of gas-phase reaction system: The gas-phase reaction system is a reduction system in which the photocatalyst is fixed on the substrate support and the mixture of CO_2 and water vapor directly reacts with the photocatalyst.
(2) Characteristics of gas-phase reaction system: Compared with the liquid-phase reaction, the gas-phase reaction is not affected by sacrificing agents, photosensitizers, solvents, and other factors, and is a relatively simple reaction system. The diffusion coefficient of CO_2 in the gas phase is about 0.1 cm^2 s^{-1}, which is about 4 orders of magnitude higher than that in the liquid phase. Therefore, in the gas-phase reaction, the mass transfer efficiency between CO_2 and photocatalyst is higher. Another advantage of gas-phase photocatalytic CO_2 reduction reaction

is that it can effectively inhibit hydrogen evolution reaction. As the reduction of H_2O to H_2 is more advantageous in thermodynamics and kinetics, the photocatalytic CO_2 reduction reaction in the liquid-phase reaction may induce hydrogen evolution and reduce the conversion rate of CO_2. Photocatalytic CO_2 reduction in gas-phase reaction can effectively solve this problem.

(3) General reaction device of gas-phase reaction system: The system for testing the photocatalytic CO_2 reduction performance using the gas-phase reaction system is generally composed of CO_2 cylinder, reactor, light source, detector, computer, and other parts [2]. Generally, the reaction is carried out in a closed air circulation system. In the experiment, a 300 W xenon lamp light source (which can also be replaced according to the specific experimental test needs) is generally used to simulate the solar radiation, and a light intensity meter can be used to adjust the appropriate light intensity. The whole reaction system is generally carried out at room temperature (special reactions can also be adjusted as required). Weigh a certain amount of the prepared photocatalyst sample and dissolve it in a specific organic solvent, then evenly coat it on filter paper or flat glass (or according to specific materials) of about a certain specification, put it into a closed system, and add 50 μl water, which is used as an electron source to annihilate holes. High-purity CO_2 (99.99%) is continuously introduced for 30 minutes to replace the air in the system so that the system is filled with saturated CO_2. The product sampling method is the same as the above method for reduction in liquid-phase photocatalytic CO_2, but no condensing device is required [3].

1.2.1.3 Detection of CO_2 Reduction Products

For a finished photocatalytic CO_2 reduction reaction, gas chromatograph (GC) can be used to detect gas-phase products (such as H_2, CO, and CH_4) [4]. The peak area of the corresponding product can be obtained after the sample extracted in the experiment is detected by GC. The yield of the product can be converted by comparing it with the curve calibrated by the standard gas [5], and the liquid-phase product can be detected by nuclear magnetic resonance.

1.2.2 The Measurement Systems of Electrocatalytic CO_2 Reduction

At present, the system for testing CO_2 reduction reaction mainly includes H-cell, flow cell, and membrane-electrode assemblies (MEA).

1.2.2.1 Electrocatalytic CO_2 Reduction Reaction Test in H-Cell

H-cell is the most common measurement system of electrocatalytic CO_2 reduction, which is a three-electrode system, as shown in Figure 1.1 [6], including a working electrode (catalyst), a counter electrode (Pt sheets or carbon rod), and a reference electrode (Ag/AgCl electrode in saturated KCl or saturated calomel electrode), as well as a proton-exchange membrane or cation-exchange membrane (Nafion 117) in the middle of the cathode and anode, which prevents the products produced by the working electrode from migrating to the surface of the anode and being oxidized.

Specifically, the first is the preparation of the working electrode. The method of preparing working electrodes differs depending on the material. Generally, there

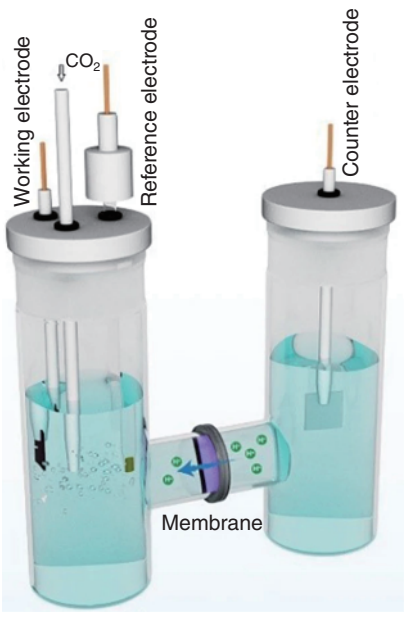

Figure 1.1 Schematic for H cell for CO_2RR. Source: Li et al. [6], with permission from John Wiley & Sons.

are two kinds of catalysts: one is materials directly grown in situ on the support, such as carbon paper, carbon cloth, foam copper, and copper foil. These catalysts can be well bonded with the substrate, which is conducive to the transmission of electrons, so the general current and stability will be better. The other is ex situ growth materials, which need to be prepared into ink and dropped onto carbon paper or glassy carbon electrode. Typically, the catalyst ink is prepared by ultrasonicating 5 mg of catalyst with 500 µl of isopropyl alcohol (or ethanol) and 10 or 20 µL of 5 wt % Nafion solutions for at least 30 minutes. And then, the catalyst ink is deposited on carbon paper or glassy carbon electrode to prepare the working electrodes with a load of 1 mg cm^{-2}. (Of course, different catalysts have different maximum loads. It can be flexibly selected according to the characteristics of materials.) It is worth noting that when the conductivity of the catalyst is poor, a certain amount of carbon black can be added during the preparation of catalyst ink to improve the conductivity of the catalyst.

The second step is about the assembly of the H-cell. Both chambers of the H-cell are equipped with electrolytes, such as 0.1 M $KHCO_3$ aqueous solution. It is worth noting that the electrolyte in cathode chamber needs to be purged with CO_2 for at least 30 minutes before electrochemical measurement.

Finally, electrocatalytic CO_2 reduction reaction is conducted on an electrochemical workstation. The catalyst is first stabilized using cyclic voltammetry (CV). Next, linear scanning voltammetry (LSV) is used to evaluate the electrocatalytic activity of the prepared samples in CO_2 or Ar-saturated 0.1 M $KHCO_3$ solution at a scanning rate of 5 mV s^{-1}. The selectivity of CO_2RR was tested using current–time (I–t) mode. The gas products are analyzed by a GC equipped with various applied potentials. Usually, the concentration of H_2 is analyzed by a thermal conductivity detector (TCD), and the concentration of CO is analyzed by a flame ionization detector (FID). The liquid products are collected at the conclusion of each electrocatalysis

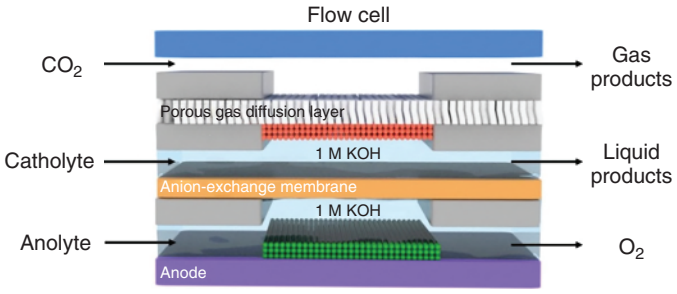

Figure 1.2 Schematic for cathode flow cell for CO_2RR. Source: Wang et al. [7] / with permission of Springer Nature.

and analyzed by the ^{1}H NMR (400 or 600 MHz). For the NMR, typically, 500 µL of catholyte is mixed with 100 µL of D_2O and 100 µl of dimethylsulfoxide (DMSO) as the internal standard.

1.2.2.2 Electrocatalytic CO_2 Reduction Reaction Test in Flow Cell

CO_2 has a low solubility in aqueous solutions, which greatly limits its mass transfer rate in electrolytes. Therefore, it has promoted the research and development of CO_2 reduction systems. In the flow cell, CO_2 can be transported directly to the surface of the catalytic electrode, significantly increasing the mass transfer rate and reaction rate.

Flow cell is an improvement on H-cell, which is also a three-chamber cell, as shown in Figure 1.2 [7]. The Nafion 117 membrane [8] or Fumasep FAB-PK-130 [7] is used to separate the anode and cathode. The electrolyte can be 0.5 M $KHCO_3$ solution, 1 M KOH solution, or other suitable electrolytes for both anode and cathode. The working electrode is usually selected from hydrophobic carbon paper, the counter electrode is a piece of Ni foam, and the reference electrode is a solid-state Ag/AgCl electrode. The flow rate of CO_2 is controlled at 20 sccm by gas mass-flow controller. The electrochemical data are measured using an electrochemical workstation. The gas-phase products are monitored in real time by gas chromatography. Similar to H-cell, the liquid-phase product is collected after one hour of electrolysis and examined by 400 or 600 MHz NMR. For specific details, please refer to Section 1.2.2.1.

1.2.2.3 Electrocatalytic CO_2 Reduction Reaction Test in MEA

To further reduce ohmic losses, MEA are designed to reduce the gap between electrodes. As shown in Figure 1.3, the cathode and anode electrodes are pressed together and sandwiched with an ion-exchange membrane in the middle, forming a zero-gap electrolytic cell [9]. The continuously humidified CO_2 gas stream is supplied directly to the cathode, and the reduction of carbon dioxide occurs at the boundary between the membrane and the cathode electrode. The cathode gas product is discharged through a simplified cold trap to collect the permeable liquid prior to the GC test. The main advantage of this device over microfluidic flow cells is that the CO_2 concentration can be increased relatively easily and significantly by pressurization, resulting in higher current densities and reaction rates.

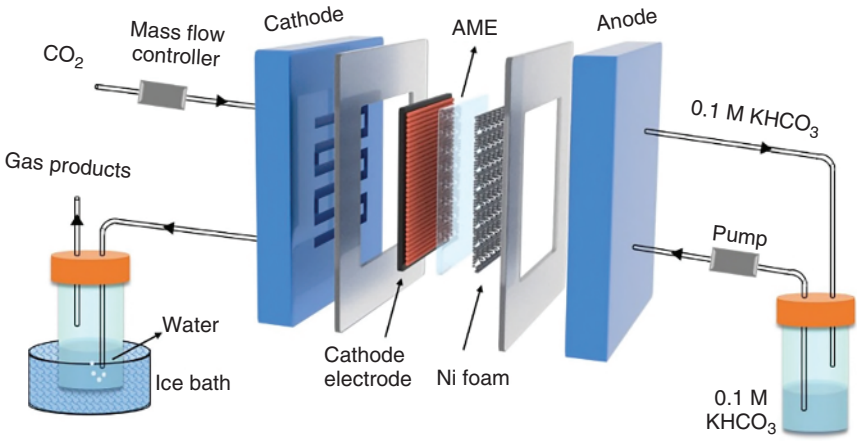

Figure 1.3 Schematic for MEA for CO_2RR. Source: Wang et al. [7] / with permission of Springer Nature.

1.2.3 The Measurement Systems of Photo-Electro-Catalytic CO_2 Reduction

1.2.3.1 Basic Device for Photocatalytic CO_2 Reduction Experiment

Photocatalytic reduction of CO_2 is usually carried out in a closed square quartz pool of a certain volume. The experiment uses a xenon lamp to simulate sunlight, and the irradiation intensity and wavelength can be selected according to the experimental requirements. The reaction device is typically composed of a three-electrode system [10], i.e. a working electrode, a counter electrode, and a reference electrode, as shown in Figure 1.4 [11].

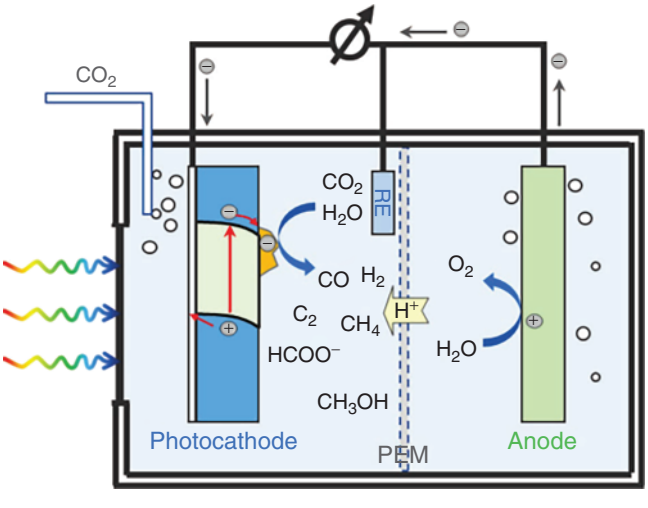

Figure 1.4 Diagram of photocatalytic CO_2 reduction reaction. Source: Li et al. [11] / with permission of John Wiley & Sons.

The most used is the prepared catalyst as a working electrode, that is, a photocathode, the counter electrode generally adopts $BiVO_4$ photoanode, the reference electrode generally adopts saturated calomel electrode, and the electrolyte is generally 0.1 M $KHCO_3$, which can be determined according to the special needs of the experiment [12]. Before proceeding with the reaction, CO_2 gas should be introduced into the system for at least 30 minutes to ensure that the CO_2 gas in the solution is saturated. Subsequently, experiments are carried out under different biases in the three-electrode system according to the experimental requirements, and the illumination time is generally two hours or set according to the experiment.

1.2.3.2 Other Devices for Photocatalytic CO_2 Reduction

In addition to the photocatalytic CO_2 reduction reaction under normal circumstances, the following devices exist. Due to photocatalysis, photocathodes and photoanodes are generally composed of p-type semiconductors and n-type semiconductors [13]. According to the configuration of the photoelectrode, the photocatalytic device can be divided into the following three types: (i) photocathodic drive battery (composed of three parts: photocathode, counter electrode, and external bias; see Figure 1.5a); (ii) photoanode-driven battery (composed of photoanode, counter electrode, and external bias; see Figure 1.5b); and (iii) photocatalytic cells jointly driven by the above two (see Figure 1.5c). Figure 1.5d is an electrode or photoelectrode-coupled photovoltaic (PV) cell for photoconversion, unlike the above three.

1.2.3.3 Detection of CO_2 Reduction Reaction Products

For the completed photocatalytic reaction, GC can be used to detect gas-phase products (such as H_2, CO, and CH_4), the sample taken in the experiment can be detected by GC, the peak area of the corresponding product can be obtained, and the yield of the product can be converted by comparing with the curve of standard gas calibration, and the liquid-phase product can be detected by nuclear magnetic resonance [14].

1.3 The Parameters for CO_2 Photo-Conversion

The main purpose of this chapter is to explain how to evaluate the advantages and disadvantages of catalysts so that experimenters can screen better catalysts.

1.3.1 The Parameters of Photocatalytic CO_2 Reduction

It is important to evaluate the photocatalytic activity, selectivity, and stability of CO_2RR catalyst with reliable performance parameters to explain the photocatalytic performance, working mechanism, and catalyst design of CO_2RR. At present, there is no uniform evaluation parameter for photocatalyst performance in the world, and standardized tests and evaluation methods need to be developed urgently. The most commonly used performance parameters are defined as follows.

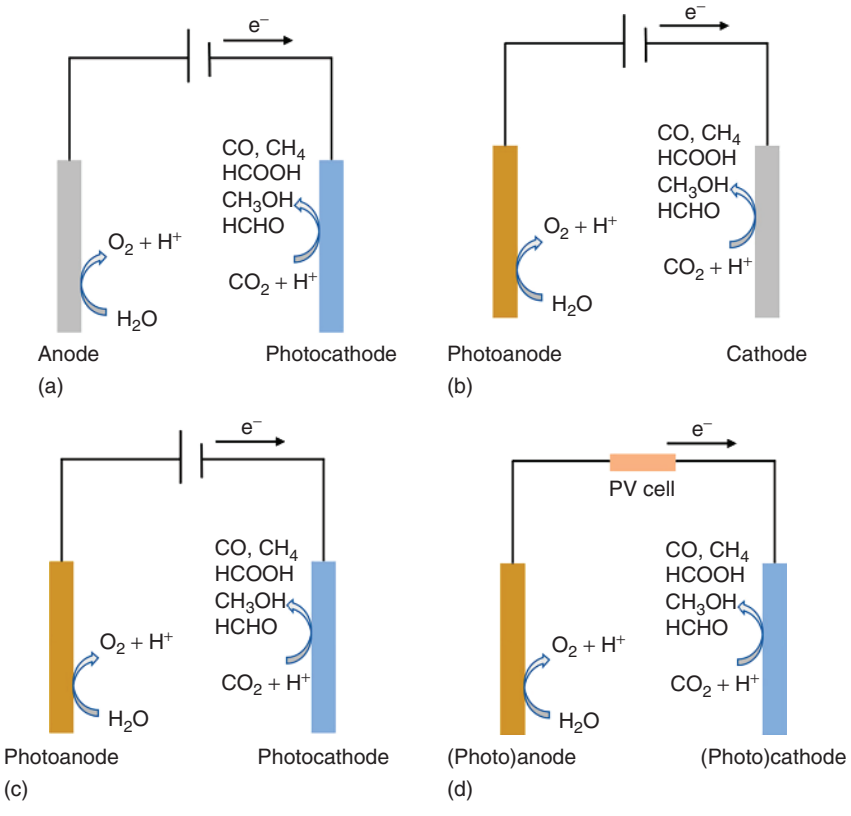

Figure 1.5 Schematic diagram of photocatalytic CO_2 reduction system including (a) photocathode-driven system, (b) photoanode-driven system, (c) photoanode and photocathode-codriven system, and (d) hybrid photosystem combining the electrode or photoelectrode with a PV cell. Source: Tang and Xiao [13] / with permission of American Chemical Society.

1.3.1.1 Evaluation Parameters of Photocatalytic CO_2 Reduction Activity

Reaction conditions have a direct impact on the photocatalytic activity, including the range and intensity of incident light, reaction temperature, reaction pressure, amount of catalyst and cocatalyst added, pH value of solution, reactor design, and structure [15, 16]. Therefore, it is a difficult task to compare the activity of photocatalysts reported under different conditions.

Generally speaking, yield is the most commonly used parameter to evaluate the activity of photocatalysts, representing the amount of target product produced by the catalyst per unit time and per unit mass. In the photocatalytic CO_2 reduction reaction, the unit of catalytic reaction yield is generally $\mu mol\ h^{-1}$ or $\mu mol\ g^{-1}\ h^{-1}$. In addition, the commonly used parameters to characterize the photocatalytic activity of the catalyst include apparent quantum yield (AQY), turnover frequency (TOF), and Solar-to-fuel energy conversion efficiency (STF).

Apparent Quantum Yield (AQY) AQY refers to the ratio of the number of electrons transferred and the number of incident photons in a reaction system at a specific monochromatic wavelength [13]. It reflects the ability to capture different energy photons during redox reactions on a certain photocatalyst, representing the light-utilization efficiency of the photocatalyst at a specific wavelength. AQY can be calculated by Eq. (1.1).

$$\mathrm{AQY} = \frac{n\,(\text{reaction electrons})}{n\,(\text{incident photons})} \tag{1.1}$$

Turnover Frequency (TOF) As shown in Eq. (1.2), TOF generally refers to the number of reactions on a unit active site in a unit time at a given temperature, pressure, and reactant ratio and a certain degree of reaction. TOF reflects the frequency of reaction at the active site of the catalyst and the intrinsic activity of the catalyst. It is considered as the most appropriate parameter to compare the activities of different catalysts.

$$\mathrm{TOF} = \frac{n\,(\text{reacted molecules per second})}{n\,(\text{active sites})} \tag{1.2}$$

However, it is difficult to determine the exact number of active sites on the photocatalyst, which hinders the application of TOF in the field of photocatalysis. Some researchers prefer to use the number of surface atoms or the number of cocatalysts to calculate TOF, that is, apparent TOF. Considering that the number of active centers may not be proportional to the surface atoms, the apparent TOF should be much lower than the actual TOF [17].

Solar-to-Fuel Energy Conversion Efficiency (STF) In addition, STF is used to evaluate the utilization ratio of photocatalysts to sunlight. For a selected product of A, the STF can be calculated by Eq. (1.3) [18].

$$\mathrm{STF} = \frac{\sum(\Delta G_0(\mathrm{A}) \times n(\mathrm{A}))}{P_{\mathrm{in}} \times t} \tag{1.3}$$

where $\Delta G_0(\mathrm{A})$ is the standard Gibbs free energy change in the process of CO_2 reduction to A, P_{in} is the input solar energy intensity and equals 100 mW cm^{-2} when Air Mass 1.5 Global (AM 1.5G) irradiation is adopted, and t is the consumed time to produce n(A) moles of A.

Photocurrent Density Photocurrent density is often used as a performance parameter in evaluating the photoelectric performance of photocatalysts. After the energy of light radiation is absorbed by the semiconductor, the valence band electrons jump to the conduction band. Under the action of a strong electric field, the conduction band electrons will move directionally to form a current, that is, photogenerated current. As shown in Eq. (1.4), photocurrent density refers to the ratio of photocurrent generated by a photoelectric electrode to the area of light irradiation under the irradiation of solar light. It is usually determined by the optical absorption, the

electron–hole pair separation efficiency, and the charge injection efficiency [19]. Therefore, the greater photocurrent response indicates that the catalyst has better charge separation and better catalytic activity.

$$\text{photocurrent density} = \frac{\text{photogenerated current}}{\text{the area of light irradiation}} \tag{1.4}$$

1.3.1.2 Evaluation Parameters of Photocatalytic CO_2 Reduction Selectivity

Photocatalytic CO_2 reduction is a reaction involving multiple electrons, which forms a variety of intermediates, making the product of CO_2 reduction diversified. Therefore, catalyst selectivity is also an important parameter to measure the quality of catalyst. The product selectivity of photocatalytic CO_2 reduction reaction can be defined as the number of electrons required to reduce the target CO_2 product compared with the number of electrons required for all reduction reactions. In general, Faraday efficiency (FE) is the most common parameter used to evaluate the selectivity of photocatalysts, quantifying the ratio of the electrons that contribute to yielding product. Hence, for a selected product of A, the corresponding FE can be calculated by Eq. (1.5). An increase in the FE of a specified product suggests an improved selectivity.

$$\text{FE(A)} = \frac{\alpha n(\text{A})F}{Q} \tag{1.5}$$

where α is the number of electrons needed to reduce CO_2 to yield one molecule of A, n(A) is the molar quantity of A, F is the Faraday constant, and Q is the total charge through the circuit in the process of generating n(A) moles of A.

In the photoelectric test, in order to evaluate the catalytic selectivity of the catalyst for a specific product, the partial photocurrent density (j_A) is also used. The j_A is calculated by multiplying the overall j_{ph} with the corresponding FE(A)

$$j_A = j_{ph} \times \text{FE(A)} \tag{1.6}$$

1.3.1.3 Evaluation Parameters of Photocatalytic CO_2 Reduction Stability

Besides the photocatalytic redox reactions, the photogenerated electrons (holes) with higher (lower) quasi-fermi energy than the thermodynamic reduction (oxidation) potential of the semiconductor can also drive the degradation or decomposition of semiconductor itself in aqueous solution under illumination, known as photocorrosion of semiconductors, which will greatly reduce the efficiency of catalytic reaction [20, 21] (Figure 1.6).

Therefore, in addition to considering the catalytic activity and selectivity, the stability of the catalytic reaction is also an important indicator to evaluate the catalyst. Long-term experiments or repeated experiments should be conducted under light to evaluate the long-term stability of photocatalyst.

1.3.2 The Parameters of Electrocatalytic CO_2 Reduction

In CO_2RR, generally, the performance of a catalyst is evaluated from the following aspects: selectivity (Faraday efficiency, here is marked as FE), activity (current density), energy efficiency (overpotential), and stability.

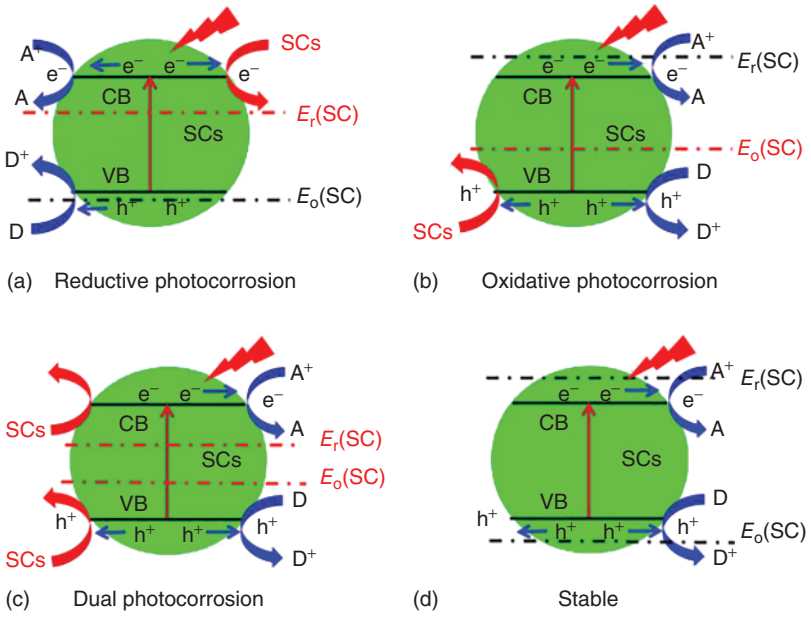

Figure 1.6 Schematic illustration of three kinds of photocorrosion: (a) oxidative photocorrosion, (b) reductive photocorrosion, (c) dual photocorrosion, and (d) stable. E_r(SC) and E_o(SC) are the thermodynamic oxidation/reduction potentials of semiconductors, respectively. Source: Li et al. [21] / with permission of American Chemical Society.

The FE means selectivity of the product. The value of FE is calculated by referring to the ratio of the transferred electric energy to the total transferred electric energy for the production of specific products. It can be calculated according to Eq. (1.7):

$$\mathrm{FE} = eF \times n/Q = eF \times n/(I \times t) \tag{1.7}$$

where e is the number of transferred electrons for each product, F the Faraday constant, Q charge, I applied current, t reaction time, and n total product.

The current density can reflect activity of catalysis. In addition, it reflects the reduction dynamics and hints at the possibility of large-scale applications. It refers to the amount of current per unit surface area (electrochemical surface area) passing through the catalyst in unit time. It can be calculated according to Eq. (1.8):

$$j_i = j_{\mathrm{total}} \times \mathrm{FE} \tag{1.8}$$

where j_i and j_{total} stand for the current density of the target product and the total current density of the reaction, respectively.

The overpotential reacts to the energy efficiency of the catalyst. The lower the overpotential, the higher the energy efficiency. The overpotential is defined as the difference between the actual potential of the reaction and the thermodynamic equilibrium potential. Overpotential is closely related to current density. When the current density increases, the overpotential also increases.

The stability of the catalyst refers to the time that the catalyst has stable activity under the conditions of use. It can usually be measured according to the I–t curve.

Operating under continuous CO_2 reduction conditions, the current density versus time behavior was evaluated by means of chronoamperometry.

1.3.3 The Parameters of Photo-Electro-Catalytic CO_2 Reduction

In PEC CO_2RR systems, photocathodes play a pivotal role, from sunlight irradiating the electrodes to product generation. The key parameters describing photocathode performance include starting potential (V_{on}), total photocurrent density (j_{ph}), FE for different products, partial photocurrent density (j_A), STF, and durability of continuous reaction under light irradiation.

1.3.3.1 Overpotential

The starting potential represents the minimum external bias required to initiate photocatalytic CO_2 reduction. The smaller the starting potential, the more likely the photocatalytic reaction is initiated, and the higher the photocathode energy conversion efficiency. Due to the competitive hydrogen evolution reaction, the starting potential does not necessarily mean the beginning of CO_2 reduction, and the current density near the starting potential shows a rather slow increase that is difficult to identify precisely. Therefore, for convenience, the starting potential is usually defined as the external bias required for the total photocurrent density to reach 0.1 mA cm^{-2} [11]. In addition, by comparing the difference between the starting potential of photoelectric CO_2 reduction and the standard redox potential of CO_2, the effective photoelectric voltage generated by the photocathode under light irradiation can be reflected, and the effective photovoltage can play a role in reducing energy consumption and improving energy utilization.

1.3.3.2 Total Photocurrent Density (j_{ph}) and Partial Photocurrent Density (j_A)

The photocurrent density is usually normalized to the exposed surface area of the photocathode in the electrolyte or the mass of the photocathode catalyst, which can reflect the reaction rate of photocatalysis and measure the catalytic activity of the photocathode. It increases rapidly after exceeding the starting potential and reaches a saturation value at a certain negative potential. The saturation photocurrent density is theoretically determined by the light absorption capacity and charge-separation efficiency of the semiconductor material, and in general, the greater saturated photocurrent brought by light indicates that the material has better photogenerated carrier generation and separation capabilities. Due to insufficient charge separation/transfer and surface catalytic reactions, the actual photocurrent density may be smaller than the theoretical value [18].

Partial photocurrent density (j_A) can be used to evaluate the catalytic activity of the photocathode on a specific product. The higher the partial photocurrent density (j_A) of the target product, the higher the selectivity of the photocathode, and the better the catalyst performance. For part of the photocurrent density of target product A, the formula is calculated as follows:

$$j_A = j_{ph} \times \mathrm{FE(A)} \tag{1.9}$$

1.3.3.3 Faraday Efficiency (FE)

In general, FE is the most common parameter used to evaluate the selectivity of photocatalyst, quantifying the ratio of the electrons that contribute to yielding product. Hence, for a selected product of A, the corresponding FE can be calculated by Eq. (1.10). An increase in the FE of a specified product suggests an improved selectivity.

$$\mathrm{FE(A)} = (\alpha n(\mathrm{A})F)/Q \tag{1.10}$$

where α is the number of electrons needed to reduce CO_2 to yield one molecule of A, n(A) is the molar quantity of A, F is the Faraday constant, and Q is the total charge through the circuit in the process of generating n(A) mole amount of A.

1.3.3.4 Solar Energy Conversion Efficiency

According to different reaction devices, STF, applied bias photon-to-current efficiency (ABPE), and half-cell STF are common parameters to evaluate the performance of the photocathodes in photoelectrochemical CO_2 reaction [11].

The STF defines the overall solar conversion efficiency of the zero-/self-biased two-electrode PEC CRR cell, and it can be calculated by Eq. (1.11).

$$\mathrm{STF} = \frac{\sum(\Delta G_0(\mathrm{A}) \times n(\mathrm{A}))}{P_{\mathrm{in}} \times t} \tag{1.11}$$

where ΔG_0(A) is the standard Gibbs free energy change in the process of CO_2 reduction to A, P_{in} is the input solar energy intensity and equals 100 mW cm^{-2} when AM 1.5G irradiation is adopted, and t is the consumed time to produce n(A) moles of A.

For some two-electrode PEC CRR cells, an external bias device (V_{bias}) is applied between the working electrode and the counter electrode to realize the photoelectric catalytic CO_2 reduction. ABPE can be used to describe the solar energy conversion efficiency of the photocathode, and it can be calculated by Eq. (1.12).

$$\mathrm{ABPE} = \frac{\sum(|j_A| \times (1.23\,\mathrm{V} - E^0(\mathrm{A}) - V_{\mathrm{bias}}))}{P_{\mathrm{in}}} \tag{1.12}$$

where j_{A} is the partial photocurrent density (j_{A}) to yield A, E^0(A) is the standard redox potential of A generated by CO_2 reduction, and P_{in} is the input solar energy intensity and equals 100 mW cm^{-2} when AM 1.5G irradiation is adopted. When the anodic reaction is water oxidation reaction, the theoretical voltage of A generated in the two-electrode PEC CRR cell is (1.23 V $- E^0$(A)).

The calculation of the solar energy conversion efficiency in half-cell STF is similar to ABPE, except that the external bias is replaced by the applied potential of the photocathode.

1.3.3.5 Apparent Quantum Yield (AQY)

AQY refers to the ratio of the number of electrons transferred and the number of incident photons in a reaction system at a specific monochromatic wavelength [13]. It reflects the ability to capture different energy photons during redox reaction on a

certain catalyst, representing the light utilization efficiency of the photocatalyst at a specific wavelength. AQY can be calculated by Eq. (1.13).

$$\mathrm{AQY} = \frac{n\,(\text{reaction electrons})}{n\,(\text{incident photons})} \tag{1.13}$$

1.3.3.6 Electrochemical Active Area (ECSA)

Electrochemical active area (ECSA) refers to the effective area involved in electrochemical reactions, which is determined by the structure and morphology of the catalyst. Photocatalysts with porous or hollow structures usually have a higher electrochemical activity specific surface area and expose richer active sites. In general, the ECSA is proportional to the catalytic performance of the photocathode catalyst. The ECSA value can be calculated from Eq. (1.14) [22].

$$\mathrm{ECSA} = \frac{\mathrm{C_{DL}}}{\mathrm{C_s}} S \tag{1.14}$$

where C_s and S are constants, representing the specific capacitance and specific surface area of the corresponding surface smoothed sample under the same conditions, respectively. CDL represents the capacitance value of the electric double layer, and the current density and sweep speed are linearly fitted by measuring the CV curve at different sweep speeds, and the resulting slope is the electrochemical electric double layer capacitance.

1.3.3.7 Electrochemical Impedance (EIS)

The Nyquist spectra from electrochemical impedance spectroscopy (EIS) can be used to evaluate the charge transfer rate between the electrode material and the electrolyte. The radius of the semicircle in the high-frequency regions corresponds to the resistance of the electrode, and the size of the radius of the semicircle in the middle and low-frequency region is used to explain the charge transfer rate at the interface between the electrode and the electrolyte, and the smaller the radius, the larger the charge transfer rate [22].

1.3.3.8 Tafel Slope (Tafel)

Tafel slope is a common indicator for evaluating photocatalytic reaction kinetics, which can be used to evaluate reaction kinetic rates and predict catalytic mechanisms. The linear part of the Tafel plot can be fitted to the Tafel equation [23]:

$$\eta = a + b \log j \tag{1.15}$$

where η represents the overpotential, b is the Tafel slope, and j is the current density.

The smaller the Tafel slope, the faster the current density increases, the smaller the overpotential change, and the higher the photocatalytic reaction kinetic rate.

1.3.3.9 Photocatalytic Stability

Besides the photocatalytic redox reactions, the photogenerated electrons (holes) with higher (lower) quasi-fermi energy than the thermodynamic reduction (oxidation) potential of the semiconductor can also drive the degradation or decomposition of semiconductor itself in aqueous solution under illumination, known

as photocorrosion of semiconductors, which will greatly reduce the efficiency of catalytic reaction [20, 21].

Therefore, in addition to considering the catalytic activity and selectivity, the stability of the catalytic reaction is also an important indicator to evaluate the catalyst.

Stability tests such as chronocurrent or chronopotentiometry can be used to assess the stability of a catalyst [24]. The chronocurrent method measures the change in the current of the working electrode with time while controlling the voltage of the working electrode. The chronopotentiometric method measures the change in the voltage of the working electrode over time while controlling the current of the working electrode. However, both the chronocurrent method and the time-potentiometric method have limitations in measuring the stability of the electrocatalyst and can only be measured at the same current or voltage. In contrast, the multistep chronocurrent method can simultaneously measure the stability of the electrocatalyst at different potentials, that is, control the voltage, from the potential step without an electrochemical reaction to the potential where the electrochemical reaction occurs while measuring the change in the current flowing through the electrode with time.

References

1 Xi, L. (2022). Controllable preparation of mesoporous Nb_2O_5 nanofibers and their photocatalytic properties for CO_2 reduction. Dissertation. University of Donghua.

2 Kang, S. (2022). Study on interface regulation and modification of CuPc/g-C_3N_4 heterojunction photocatalyst for CO_2 reduction. Dissertation. Heilongjiang University.

3 Xi, C. (2022). Preparation of carbon nitride/metal chalcogenides and their photocatalytic properties for CO_2 reduction. Dissertation. Heilongjiang University.

4 Wang, J., Hao, C., Wei, D. et al. (2022). Ultrasonic assisted preparation of $Cs_2AgBiBr_6/Bi_2WO_6S$ heterojunction for visible light photocatalytic CO_2 reduction. *Chin. J. Catal.* 43 (10): 2606–2614.

5 Hong, L. (2022). Design and synthesis of Ti_3C_2 based composite photocatalytic materials and study on the mechanism of CO_2 photocatalytic reduction. Dissertation. Shanghai University of Electric Power.

6 Li, C., Ji, Y., Wang, Y. et al. (2023). Applications of metal-organic frameworks and their derivatives in electrochemical CO_2 reduction. *Nano-Micro Lett.* 15 (1): 113.

7 Wang, P., Yang, H., Tang, C. et al. (2022). Boosting electrocatalytic CO_2-to-ethanol production via asymmetric C–C coupling. *Nat. Commun.* 13: 3754.

8 Zhang, Y., Jang, H., Zhang, W. et al. (2022). Single-atom Sn on tensile-strained ZnO nanosheets for highly efficient conversion of CO_2 into formate. *Adv. Energy Mater.* 12 (45): 2202695.

9 Ma, D., Jin, T., Xie, K. et al. (2021). An overview of flow cell architectures design and optimization for electrochemical CO_2 reduction. *J. Mater. Chem. A* 9: 20897–20918.

10 Pan, W., Li, C., and Guo, R. (2022). Progress in photocatalytic CO_2 reduction technology. *J. Huazhong Univ. Sci. Technol.* 11: 1–13.

11 Li, D., Yang, K., Lian, J. et al. (2022). Powering the world with solar fuels from photoelectrochemical CO_2 reduction: basic principles and recent advances. *Adv. Energy Mater.* 12 (31): 2201070.

12 Lin, H. (2021). Preparation of bismuth sulfide based heterojunction materials and their photocatalytic reduction of carbon dioxide. Dissertation. Lan Zhou University.

13 Tang, B. and Xiao, F.X. (2022). An overview of solar-driven photoelectrochemical CO_2 conversion to chemical fuels. *ACS Catal.* 12 (15): 9023–9057.

14 Yun, C. (2021). Preparation of Fe based MOF derived composites and their photocatalytic reduction of carbon dioxide. Dissertation. Lan Zhou University.

15 Li, X., Yu, J., and Low, J. (2015). Engineering heterogeneous semiconductors for solar water splitting. *J. Mater. Chem. A* 3 (6): 2485.

16 Li, K., An, X., Park, K.H. et al. (2014). A critical review of CO_2 photoconversion: catalysts and reactors. *Catal. Today* 224: 3–12.

17 You, F. (2021). Design of hollow multi shell heterostructures and their photocatalytic properties for CO_2 reduction. Dissertation. University of Chinese Academy of Sciences.

18 Zhang, D. (2021). Preparation of ZIF-8 matrix composites and their photoelectric catalysis for CO_2 to formate. Dissertation. Taiyuan University of Technology.

19 Jian, J. and Sun, J. (2020). A review of recent progress on silicon carbide for photoelectrochemical water splitting. *Solar RRL* 4 (7): 2000111.

20 Li, X., Yu, J., Wageh, S. et al. (2016). Graphene in photocatalysis: a review. *Small* 12 (48): 6640–6696.

21 Li, X., Jiaguo, Y., Jaroniec, M. et al. (2019). Cocatalysts for selective photoreduction of CO_2 into solar fuels. *Chem. Rev.* 119 (6): 3962–4179.

22 Hou, J. (2022). Preparation of copper modified MOF material and its photoelectric catalytic reduction of CO_2. Dissertation. Lan Zhou University.

23 Wu, A.P., Gu, Y., Yang, B.R. et al. (2020). Porous cobalt/tungsten nitride polyhedra as efficient bifunctional electrocatalysts for overall water splitting. *J. Mater. Chem. A* 8 (43): 22938–22946.

24 Shen, Q., Ma, J., Huang, X. et al. (2017). Enhanced carbon dioxide conversion to formate on a multi-functional synergistic photoelectrocatalytic interface. *Appl. Catal., B* 219: 45–52.